Research Article Vol. 3, No. 7 / 15 July 2020 / OSA Continuum 1958

OSA CONTINUUM

Optical analysis of homocysteine metabolites using vibrational spectroscopy

MINGZHOU CHEN,[1,*] LISA STROTHER,[2] GAYLE H. DOHERTY,[2] AND KISHAN DHOLAKIA[1,3]

[1] SUPA, School of Physics & Astronomy, University of St. Andrews, St. Andrews, Fife, KY16 9SS, UK
[2] School of Psychology and Neuroscience, University of St. Andrews, St. Andrews, Fife, KY16 9TS, UK
[3] Department of Physics, College of Science, Yonsei University, Seoul 03722, South Korea
[*] mingzhou.chen@st-andrews.ac.uk

Abstract: Homocysteine (HCy) is a sulphur-containing amino acid that correlates with several maladaptive health conditions, including an enhanced risk of cardiovascular and neurodegenerative diseases. Detection of HCy and its potentially pathogenic metabolites are studied here for the first time, to the first of our knowledge, using Raman spectroscopy. This study shows that different HCy metabolites have distinct Raman spectra and that the limits of detection reach the sub-mM level for these compounds. This investigation paves the way for photonics–based approaches for detection of HCy–related fluids as predictive biomarkers of disease in blood, which would assist in early intervention for improved clinical outcomes.

1. Introduction

Homocysteine (HCy) is a sulphur–containing amino acid produced as a by–product of the S–adenosyl methionine cycle. Under normal circumstances, generated HCy is either recycled back to form methionine via a folate–dependent pathway, or broken down for renal excretion following condensation with serine to form cystothionine [1]. As accepted widely, normal plasma HCy levels are 5-15 μM. Elevated circulating levels of HCy (>15 μM) have been prospectively linked to an enhanced risk of cardiovascular and neurodegenerative disease [2]. Furthermore, the metabolic disorder, homocysteinuria, occurs in individuals with homozygous null mutations in genes encoding either methyl tetrafolate reductase or cystathionine β–synthase. These patients have vastly elevated HCy levels in the range of 100–500μM [3] and present with a spectrum of symptoms including skeletal abnormalities [4], cardiovascular disease, ophthalmological abnormalities and neuropsychiatric disorders [5]. Early intervention with a low-methionine diet and high dose folate and B vitamin therapy can halt, and indeed reverse, a number of these symptoms.

In addition to HCy *per se*, its metabolites have been observed to have deleterious effects on health and wellbeing. Homocysteine thiolactone (HT) has been linked to deficits in vascular function [6], and the activity of homocysteine thiolactonase, the enzyme that hydrolyses HT to HCy, for breakdown and excretion, is reduced in Alzheimer's Disease patients [7] linking increased HT levels to neurodegeneration. Administration of an oxidised metabolite of HCy, homocysteic acid (HA) to rodents induces increased arterial pressure and heart rate [8] and HA also causes Aβ1-42 accumulation in neurons linking it to the pathogenesis of Alzheimer's Disease [9]. Together these findings imply that not only HCy, but also substances that are known metabolic fates of this amino acid, are linked to the pathogenesis of cardiovascular and neurodegenerative diseases.

To date the relative amounts of HCy and its potentially pathogenic metabolites have not been investigated in either patient samples or under laboratory conditions. One of the reasons for

#397780 https://doi.org/10.1364/OSAC.397780
Journal © 2020 Received 18 May 2020; revised 16 Jun 2020; accepted 17 Jun 2020; published 7 Jul 2020

OSA CONTINUUM

this lack of data rests with the difficulty in accurately discriminating between and detecting these substances. HCy levels within blood can change markedly and rapidly following sample collection. As HCy is released from cellular components, levels increase at the rate of 10% per hour following blood sampling and thus rapid separation of blood cells from plasma and serum is required [10]. Following separation, plasma HCy levels are stable and a variety of techniques can be used for determination of levels including mass spectroscopy [11] and enzymatic assays [12]. HT can be measured using HPLC or GS/MS [13] although routine blood sampling for this and HA is not currently available. HA can be measured by liquid mass spectrometry [14] or GS/MS [15].

As the potential for HCy metabolites to mediate HCy–linked neurotoxicity and cardiovascular dysfunction emerges, the need to simultaneously measure HCy, HT and HA in a single sample presents itself as a key challenge. To achieve this goal, it is necessary to develop an assay where the three metabolites can be identified and measured. In this paper, we explore the powerful label-free approach of Raman spectroscopy to address this question. Raman analysis generates a chemical fingerprint of a sample, and has previously been used successfully on cells [16,17], bacteria [18–20] and tissue [21].

Importantly, to date, there are very few studies of Raman analysis on these important metabolites in the literature [22] while a few others rely on alternative techniques, such as terahertz spectroscopy and near-infrared fluorescence spectroscopy [23–25]. Here, we address this and use Raman analysis to acquire unique spectra from each of these metabolites, monitor metabolite concentrations and set limits on detection. In particular, we use a recently developed variant of Raman analysis, wavelength modulated Raman spectroscopy (WMRS) [16,17,26], and compare that with a standard Raman approach. WMRS allows us to remove any obscuring background fluorescence without the need to use any polynomial fitting. This is mainly based on the premise that the background fluorescence does not change when the excitation laser wavelength is tuned over a small range of 1.5 nanometres, while the Raman peaks do change. The use of WMRS is shown to lead to an increased sensitivity for detection of HCy and its pathogenic metabolites. Our work will ultimately lead to label-free optical analysis for these important metabolites.

2. Methods

2.1. Preparation of homocysteine metabolite solutions

All chemical samples were obtained from Sigma Aldrich UK and exist as a 50:50 ratio of the D– and L– stereoisomers. Aliquots of each chemical were weighed and stored at −20 °C with desiccant prior to experiments. Immediately before performing Raman spectroscopy, HCy was prepared as a 200 mM stock in 0.15 M NaCl solution which does not have distinctive Raman peaks between 500 cm^{-1} and 2000 cm^{-1} [27,28]. Saline with a physiological concentration of NaCl was used to dissolve HCy as this compound exhibits a salting-in behavior in physiological fluids allowing preparation of a higher concentration stock than could be obtained in water alone [29]. This stock was then further diluted in 0.15 M NaCl to give experimental samples at 100 mM, 80 mM, 50 mM and 20 mM. Both HT and HA were prepared as a 200 mM stock in dH_2O, and further diluted to give 100 mM, 80 mM, 50 mM, 20 mM, 10 mM and 5 mM samples. A volume of 20 μL sample solution was loaded into a well formed by one thick quartz slide (1 mm thickness), one thin quartz slide ($\sim$ 170μm thickness) and a vinyl spacer with a central hole.

2.2. Raman spectroscopy

The standard and wavelength modulated Raman spectroscopy was performed with a wavelength tunable Ti:Sapphire laser (Spectra-Physics 3900s, 1 W@785 nm) to excite Raman photons which were collected by a monochromator (Shamrock SR-303i, Andor Technology) and a

OSA CONTINUUM

thermoelectrically cooled CCD camera (Newton, Andor Technology) [16]. An oil immersion objective (Nikon, NA0.9/50X) focused the laser onto the sample, delivering a power of 150 mW to the sample solution. We verified that this laser dosage did not cause any damage by continuously acquiring Raman spectra from sample solutions for half an hour, upon which no change was found in all acquired spectra.

For the system operating in standard Raman mode, we acquired at least five spectra from each sample solution by setting the tunable Ti:Sapphire laser to a fixed wavelength of 785 nm. An acquisition time of 28 s was used to record a single spectrum from differing concentrations of HCy, HT and HA in solution.

Wavelength modulated Raman spectra from the sample solution were obtained with exactly the same system with only a slight modification of procedure and laser operation. Five Raman spectra were recorded from the sample solution at different excitation wavelengths for a total modulation range of $\Delta\lambda = 1$nm. We note that a longer overall acquisition time is needed for WMRS as the same acquisition time of 28s was used for each individual spectrum. Principal component analysis (PCA) was used to analyze these five spectra, with each wavelength step as a parameter, to produce a modulated Raman spectrum with essentially all fluorescence background being suppressed [16,17]. As a result, all Raman peaks are indicated by the zero crossing points in the resulting modulated Raman spectrum.

2.3. Data analysis

Raman spectra in the region of 600 cm^{-1} to 1800 cm^{-1} were used for subsequent analysis. Since the intensity of the Raman peak varies depending on the concentration of sample solution, we monitored the intensity of the most significant Raman peak (670 cm^{-1}, 1050 cm^{-1} and 690 cm^{-1} in HCy, HA and HT Raman spectra respectively). For the Standard Raman spectrum, we directly calculate the peak intensity from the baseline at the peak position. For the wavelength modulated Raman spectrum, the peak intensity was calculated from the peak–to–valley value at the zero crossing point.

3. Results

HCy, HA and HT show unique Raman spectra

The most critical step in the study was to determine whether the three metabolites had unique Raman spectra that could be readily distinguished from one another. Figure 1 shows standard Raman spectra and WMR spectra from HCy, HA and HT solutions. Distinct Raman fingerprints can be clearly observed at the peaks in standard Raman spectra or at the zero crossing points in WMRS. Different Raman fingerprints are shown for HCy (Fig. 1(a) and (b)), HA (Fig. 1(c) and (d)) and HT (Fig. 1(e) and (f)). Typical Raman peaks from our measurements are shown in Table 1.

Table 1. Typical Raman peaks in HCy, HA and HT solutions. A characteristic Raman peak for each solution were indicated by the bold-font number.

	Typical Raman peak positions (cm^{-1})
HCy	**670**, 756, 865, 1086, 1360, 1420, 1448
HA	820, **1050**, 1200, 1430
HT	**690**, 745, 982, 1190, 1395, 1465

OSA CONTINUUM

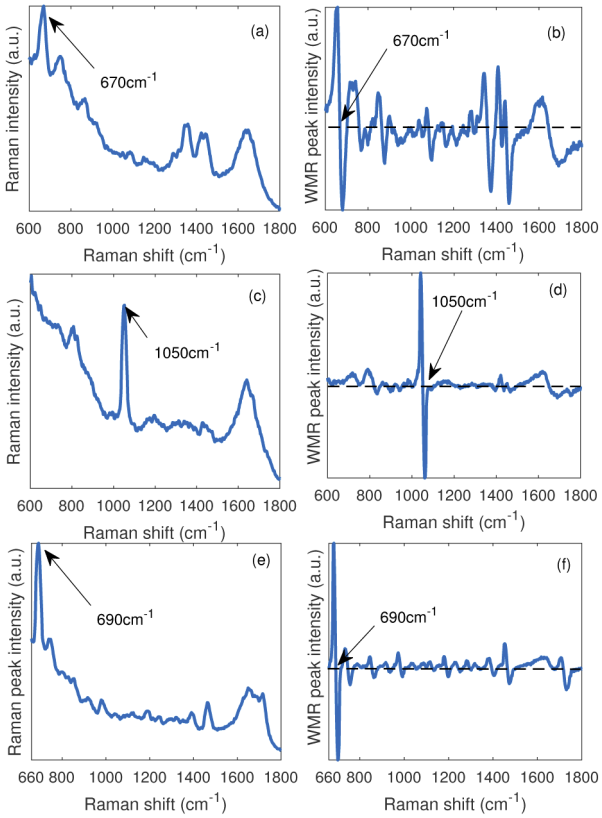

Fig. 1. Standard Raman spectra (a, c, e) and wavelength modulated Raman spectra (b, d, f) of HCy solution at a concentration of 0.2 M, HA solution with a concentration of 0.1 M and HT solution at a concentration of 0.1 M. Arrows indicate the most significant Raman peaks at 670 cm^{-1}, 1050 cm^{-1} and 690 cm^{-1} for HCy, HA and HT respectively. The dashed line in (b), (d), and (f) shows the zero intensity in wavelength modulated Raman spectra.

3.1. Raman peak intensity correlates with the concentrations of HCy, HA or HT in solution

As would be expected, our data demonstrate that the intensity of Raman peaks varies depending on the concentration of solution. Here we focus on the most significant Raman peak of spectra of HCy, HA or HT solutions in order to monitor the peak intensity relative to the concentration of sample solutions and set a limit of detection for the current system. From the spectrum region of 600–1800 cm^{-1}, three most significant Raman peaks at 670 cm^{-1}, 1050 cm^{-1}, and 690 cm^{-1} were selected as characteristic Raman peaks for HCy, HA and HT solutions respectively.

Figure 2 shows the relationship between these characteristic Raman peak intensities and the concentrations of the metabolites in solution. The linearity between the Raman peak intensity and the concentration can be clearly observed for all three compounds investigated. Clearly, WMRS shows an improvement in measuring these Raman peaks at different concentrations.

We also evaluated the signal to noise ratio (SNR) for each measurement by taking the ratio of measured characteristic Raman peak intensity value to the standard deviation of the Raman free spectral region (noise region) between 1925 cm^{-1} and 1985 cm^{-1}. For the standard Raman spectra, we take the first differential and then evaluate the SNR in the same way. In Fig. 3 we see that the SNR has been enhanced by a factor of two for the WMR spectra due to the suppression

OSA CONTINUUM

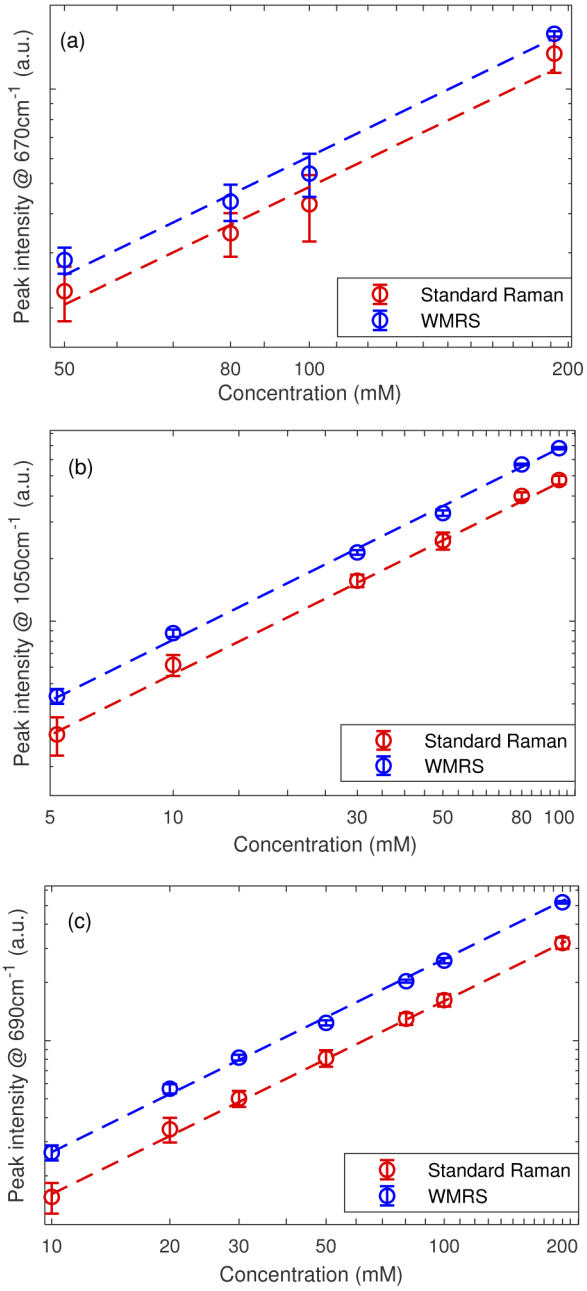

Fig. 2. Raman peak intensities as a function of concentrations for (a) HCy, (b) HA and (c) HT solution with both axes on the log scale. Blue stars show the peak intensities of wavelength modulation Raman spectra and red circles show the peak intensities of standard Raman spectra at 670 cm^{-1}, 1050 cm^{-1} and 690 cm^{-1}. Dashed lines shows the linear fits from the experimental data.

of the fluorescence background. The sensitivity of the concentration prediction ability can be defined as the slope (β) of these linear fitted curves, which also show an enhancement by a factor of two for the WMR spectra. Therefore, our experimental results indicate that WMRS improves the prediction of concentration for these key metabolites as a result of the fluorescent background suppression associated with the technique. Furthermore, the theoretical detection limit can be estimated by $1/\beta$, which is the concentration when SNR is approaching to 1. In our study, the theoretical detection limits for HCy, HA and HT using WMRS are 3.704, 0.719 and 0.724 mM respectively.

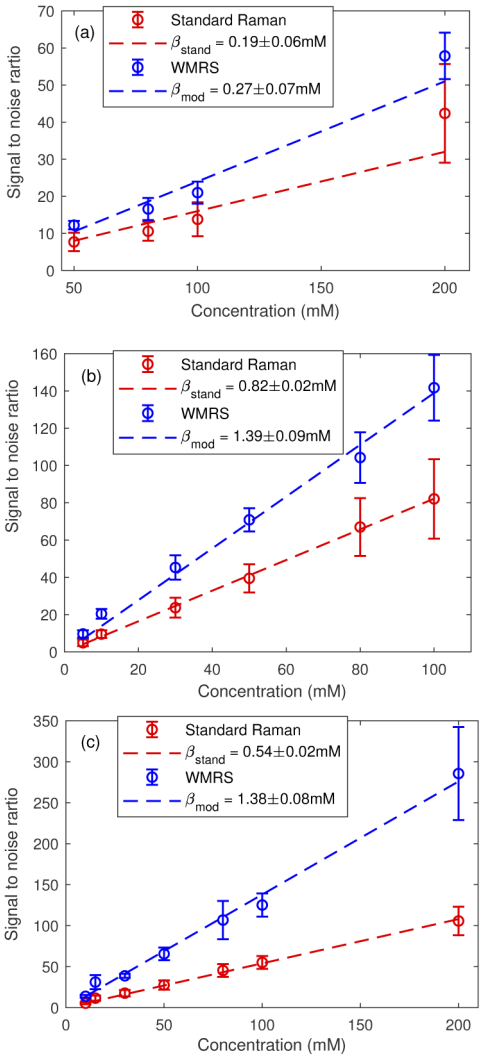

Fig. 3. Comparison of signal to noise ratio between standard Raman spectra and WMR spectra obtained from (a) HCy, (b) HA, and (c) HT solution. Dashed lines show the linear fits from the experimental data and the slopes of the fitted lines are indicated by the value of β.

OSA CONTINUUM

4. Conclusions and discussions

In this study, our primary objective was to determine whether key metabolites that have been shown to link HCy dysregulation to cardiovascular and neurodegenerative disease [2] have unique Raman spectra. We have confirmed this by recording unique Raman fingerprints for each metabolite suggesting that Raman spectroscopy offers the potential to rapidly and accurately detect HCy, HA and HT in solution. Furthermore, we have demonstrated a concentration-dependent change in the intensity of the major peak for each metabolite indicating that we can determine the concentration as well as the presence of each of these metabolites.

We demonstrated that WMRS exhibited enhanced sensitivity in detecting these solutions when compared to standard Raman and this is in keeping with previous studies demonstrating that WMRS can give greater sensitivity in the detection of biological parameters. Restricted by the laser power and the focusing lens used in our system, the low limits of detection are typically below 4 mM for each metabolite studied. Here, those prominent Raman peaks at 670 cm^{-1} and 690 cm^{-1} from the HCy and HT are strongly related to the (C-S) stretching mode and (C-S) trans respectively in the molecues [30]. The Raman peak at 1050 cm^{-1} indicates the SO_3 stretching in HA molecues [31]. As each metabolite shows a unique Raman fingerprint, it is possible to measure the concentration of these three metabolites simultaneously in a solution. This implies that determining the relative level of each in biological samples such as blood is possible if the these fingerprints are not overwhelmed by those from other contents.

It has long been established that HCy is a prospective risk factor for the development of cardiovascular and neurodegenerative conditions, having been identified as increasing future risk of heart disease in the 1970s [32] and of Alzheimer's Disease in 2002 [33]. Despite these findings, vitamin-based therapies to reduce HCy burden have failed to show beneficial effects for patients on either cardiovascular [34] or cognitive parameters [35]. The reasons for this are unclear. It is possible that the damage caused by HCy pre-dates the onset of symptoms and therefore lowering levels after the disease process has begun offers no patient benefit. Indeed, HCy levels are not routinely clinically measured [36] and therefore early identification of patients who would benefit from intervention to lower HCy levels is difficult. There is emerging data that early intervention to lower HCy prior to disease onset could be beneficial. Thus in high-risk patients, such as those with elevated cardiovascular disease risk due to rheumatoid arthritis, HCy-lowering therapies using folate resulted in decreased carotid intima-media thickness, an indicator of future cardiovascular events [37]. It will be interesting to see if further longitudinal studies provide clear evidence that this decrease in carotid intima-media thickness translates to a verified decrease in cardiovascular events in these patients. Similarly, vitamin B supplementation given to hyperhomocysteinemic patients (55-95 yrs) who do not show evidence of Alzheimer's disease, resulted in decreased HCy levels correlated to the enhanced cognitive function [38]. This again suggests that early intervention, prior to the onset of clinically relevant cognitive decline could be protective. Crucially all of this evidence focused on HCy alone and did not consider HT or HA, both of which have maladaptive effects in the nervous system. It is plausible that in studies with no patient benefit observed that HA and HT levels are not significantly altered following B vitamin administration and that additional pharmacological interventions may be required to significantly affect these metabolites.

In these experiments, our limit of detection is 10-fold higher than that required for use of such Raman analysis in a physiological setting, which is smaller than 500 μM. However, with further refinement and enhancement, for example, using a surface-enhanced Raman approach, our method shows excellent potential to approach the physiologically meaningful range. In future, it paves the way to rapidly monitor the levels of these important metabolites, either as a single compound or in a mixture, in a clinical setting. Our work also paves the way for future studies using either enhancement techniques (*e.g.* Surface enhanced Raman analysis) [39] performed on

OSA CONTINUUM

microfluidic or paper based substrates that would may ultimately lead to label free point-of-care analysis for these compounds.

Funding

European Union FAMOS project (FP7-ICT-317744); Engineering and Physical Sciences Research Council (EP/P030017/1).

Acknowledgements

We thank the UK Engineering and Physical Sciences Research Council (EP/P030017/1), the European Union FAMOS project (FP7-ICT-317744), and the RS MacDonald Charitable Trust for funding.

Disclosures

The authors declare that there are no conflicts of interest related to this article.

References

1. V. Vitvitsky, M. Thomas, A. Ghorpade, H. E. Gendelman, and R. Banerjee, "A Functional Transsulfuration Pathway in the Brain Links to Glutathione Homeostasis," J. Biol. Chem. **281**(47), 35785–35793 (2006).
2. G. H. Doherty, "Homocysteine and Parkinson's Disease: A Complex Relationship," J. Neurol. Disord. **1**(1), 107 (2013).
3. M. Amores-Sánchez and M. A. Medina, "Methods for the determination of plasma total homocysteine: a review," Clin. Chem. Lab. Med. **38**(3), 199–204 (2000).
4. J. B. J. van Meurs, R. A. M. Dhonukshe-Rutten, S. M. F. Pluijm, M. van der Klift, R. de Jonge, A. G. Lindemans, and J. Uitterlinden, "Homocysteine Levels and the Risk of Osteoporotic Fracture," N. Engl. J. Med. **350**(20), 2033–2041 (2004).
5. N. A. Carson, D. C. Cusworth, C. E. Dent, C. M. Field, D. W. Neill, and R. G. Westall, "Homocystinuria: A New Inborn Error of Metabolism Associated With Mental Deficiency," Arch. Dis. Child. **38**(201), 425–436 (1963).
6. V. Zivkovic, V. Jakovljevic, O. Pechanova, I. Srejovic, J. Joksimovic, D. Selakovic, N. Barudzic, and D. M. Djuric, "Effects of DL-Homocysteine Thiolactone on Cardiac Contractility, Coronary Flow, and Oxidative Stress Markers in the Isolated Rat Heart: The Role of Different Gasotransmitters," BioMed Res. Int. **2013**, 1–9 (2013).
7. N. Akchiche, C. Bossenmeyer-Pourie, R. Kerek, N. Martin, G. Pourie, V. Koziel, D. Helle, J. M. Alberto, S. Ortiou, J. M. Camadro, T. Leger, J. L. Gueant, and J. L. Daval, "Homocysteinylation of neuronal proteins contributes to folate deficiency-associated alterations of differentiation, vesicular transport, and plasticity in hippocampal neuronal cells," FASEB J. **26**(10), 3980–3992 (2012).
8. C. P. Yardley, J. M. Andrade, and L. C. Weaver, "Evaluation of cardiovascular control by neurons in the dorsal medulla of rats," J. Auton. Nerv. Syst. **29**(1), 1–11 (1989).
9. T. Hasegawa, W. Ukai, D.-G. Jo, X. Xu, M. P. Mattson, M. Nakagawa, W. Araki, T. Saito, and T. Yamada, "Homocysteic acid induces intraneuronal accumulation of neurotoxic Aβ42: Implications for the pathogenesis of Alzheimer's disease," J. Neurosci. Res. **80**(6), 869–876 (2005).
10. F. Wolff, P. Gausset, and J. Vanderpas, "Better stability of total homocysteine measurement with sodium fluoride than with edta," Clin. Lab. **51**(5-6), 275–278 (2005).
11. K. Tuschl, O. A. Bodamer, W. Erwa, and A. Mühl, "Rapid analysis of total plasma homocysteine by tandem mass spectrometry," Clin. Chim. Acta **351**(1-2), 139–141 (2005).
12. Y. Tan, X. Sun, L. Tang, N. Zhang, Q. Han, M. Xu, X. Tan, X. Tan, and R. M. Hoffman, "Automated Enzymatic Assay for Homocysteine," Clin. Chem. **49**(6), 1029–1030 (2003).
13. G. Chwatko and H. Jakubowski, "The determination of homocysteine–thiolactone in human plasma," Anal. Biochem. **337**(2), 271–277 (2005).
14. S. Kim, M. Kim, Y. Kim, S. Ahn, K. Kim, K. Kim, W. Kim, J. Lee, J. Cho, and B. Yoo, "Differential levels of L–homocysteic acid and lysophosphatidylcholine (16:0) in sera of patients with ovarian cancer," Oncol. Lett. **8**(2), 566–574 (2014).
15. C. Santhoshkumar, J. Deutsch, J. Kolhouse, K. Hassell, and J. Kolhouse, "Measurement of excitatory sulfur amino acids cysteine sulfinic acid, cysteic acid, homocysteine sulfinic acid, and homocysteic acid in serum by stable isotope dilution gas chromatography-mass spectrometry and selected ion monitoring," Anal. Biochem. **220**(2), 249–256 (1994).
16. M. Chen, N. McReynolds, E. C. Campbell, M. Mazilu, J. Barbosa, K. Dholakia, and S. J. Powis, "The Use of Wavelength Modulated Raman Spectroscopy in Label-Free Identification of T Lymphocyte Subsets, Natural Killer Cells and Dendritic Cells," PLoS One **10**(5), e0125158 (2015).

OSA CONTINUUM

17. L. Woolford, M. Chen, K. Dholakia, and C. S. Herrington, "Towards automated cancer screening: Label-free classification of fixed cell samples using wavelength modulated Raman spectroscopy," J. Biophotonics **11**(4), e201700244 (2018).
18. I. Gusachenko, M. Chen, and K. Dholakia, "Raman imaging through a single multimode fibre," Opt. Express **25**(12), 13782 (2017).
19. V. O. Baron, M. Chen, S. O. Clark, A. Williams, R. J. H. Hammond, K. Dholakia, and S. H. Gillespie, "Label-free optical vibrational spectroscopy to detect the metabolic state of M. tuberculosis cells at the site of disease," Sci. Rep. **7**(1), 9844 (2017).
20. V. O. Baron, M. Chen, B. Hammarstrom, R. J. H. Hammond, P. Glynne-Jones, S. H. Gillespie, and K. Dholakia, "Real-time monitoring of live mycobacteria with a microfluidic acoustic-Raman platform," Commun. Biol. **3**(1), 236 (2020).
21. M. Chen, J. Mas, L. H. Forbes, M. R. Andrews, and K. Dholakia, "Depth-resolved multimodal imaging: Wavelength modulated spatially offset Raman spectroscopy with optical coherence tomography," J. Biophotonics **11**(1), e201700129 (2018).
22. X. Zhang, Z. Yang, W. Li, H. Jia, and J. Wu, "The structure of DL-homocysteic acid in D_2O solution," Spectrosc. Spect. Anal. **20**(5), 638–640 (2000).
23. F. Kong, R. Liu, R. Chu, X. Wang, K. Xu, and B. Tang, "A highly sensitive near-infrared fluorescent probe for cysteine and homocysteine in living cells," Chem. Commun. **49**(80), 9176–9178 (2013).
24. T. Li, H. Ma, Y. Peng, X. Chen, Z. Zhu, X. Wu, T. Kou, B. Song, S. Guo, L. Liu, and Y. Zhu, "Gaussian numerical analysis and terahertz spectroscopic measurement of homocysteine," Biomed. Opt. Express **9**(11), 5467 (2018).
25. L. Wang, X. Wu, Y. Peng, Q. Yang, X. Chen, W. Wu, Y. Zhu, and S. Zhuang, "Quantitative analysis of homocysteine in liquid by terahertz spectroscopy," Biomed. Opt. Express **11**(5), 2570 (2020).
26. A. C. De Luca, M. Mazilu, A. Riches, C. S. Herrington, and K. Dholakia, "Online fluorescence suppression in modulated raman spectroscopy," Anal. Chem. **82**(2), 738–745 (2010).
27. W. Möller and R. Kaiser, "Impurity induced Raman spectra of NaCl and KCl crystals with various monovalent impurities," Phys. Status Solidi B **50**(1), 155–169 (1972).
28. I. Đuričković, M. Marchetti, R. Claverie, P. Bourson, J.-M. Chassot, and M. D. Fontana, "Experimental Study of NaCl Aqueous Solutions by Raman Spectroscopy: Towards a New Optical Sensor," Appl. Spectrosc. **64**(8), 853–857 (2010).
29. R. Ragone, "Homocystine solubility and vascular disease," FASEB J. **16**(3), 401–404 (2002).
30. Z. Movasaghi, S. Rehman, and I. U. Rehman, "Raman Spectroscopy of Biological Tissues," Appl. Spectrosc. Rev. **42**(5), 493–541 (2007).
31. S. Sato, S. Higuchi, and S. Tanaka, "Identification and Determination of Oxygen-Containing Inorganosulfur Compounds by Laser Raman Spectrometry," Appl. Spectrosc. **39**(5), 822–827 (1985).
32. K. S. McCully and R. B. Wilson, "Homocysteine theory of arteriosclerosis," Atherosclerosis **22**(2), 215–227 (1975).
33. S. Seshadri, A. Beiser, J. Selhub, P. F. Jacques, I. H. Rosenberg, R. B. D'Agostino, P. W. Wilson, and P. A. Wolf, "Plasma Homocysteine as a Risk Factor for Dementia and Alzheimer's Disease," N. Engl. J. Med. **346**(7), 476–483 (2002).
34. R. Clarke, J. Halsey, S. Lewington, E. Lonn, J. Armitage, J. E. Manson, K. H. Bønaa, J. D. Spence, O. Nygård, R. Jamison, J. M. Gaziano, P. Guarino, D. Bennett, F. Mir, R. Peto, R. Collins, and B-Vitamin Treatment Trialists' Collaboration, "Effects of lowering homocysteine levels with b vitamins on cardiovascular disease cancer, and cause-specific mortality: Meta-analysis of 8 randomized trials involving 37 485 individuals," Arch. Intern. Med. **170**(18), 1622–1631 (2010).
35. R. Clarke, D. Bennett, S. Parish, S. Lewington, M. Skeaff, S. J. Eussen, C. Lewerin, D. J. Stott, J. Armitage, G. J. Hankey, E. Lonn, J. D. Spence, P. Galan, L. C. de Groot, J. Halsey, A. D. Dangour, R. Collins, and F. Grodstein, "Effects of homocysteine lowering with B vitamins on cognitive aging: meta-analysis of 11 trials with cognitive data on 22,000 individuals," Am. J. Clin. Nutr. **100**(2), 657–666 (2014).
36. J. Nichols, "Testing for homocysteine in clinical practice," Nutr. Health **23**(1), 13–15 (2017).
37. X. Qin, M. Xu, Y. Zhang, J. Li, X. Xu, X. Wang, X. Xu, and Y. Huo, "Effect of folic acid supplementation on the progression of carotid intima-media thickness: A meta-analysis of randomized controlled trials," Atherosclerosis **222**(2), 307–313 (2012).
38. D. Cheng, H. Kong, W. Pang, H. Yang, H. Lu, C. Huang, and Y. Jiang, "B vitamin supplementation improves cognitive function in the middle aged and elderly with hyperhomocysteinemia," Nutr. Neurosci. **19**(10), 461–466 (2016).
39. B. Sharma, R. R. Frontiera, A.-I. Henry, E. Ringe, and R. P. Van Duyne, "SERS: Materials, applications, and the future," Mater. Today **15**(1-2), 16–25 (2012).